

## Experimental study of the He stopping power into $\text{Al}_2\text{O}_3$ films

E.D. Cantero <sup>a</sup>, R.C. Fadanelli <sup>b</sup>, M. Behar <sup>b,\*</sup>, L.C.C.M. Nagamine <sup>c</sup>, G.H. Lantschner <sup>a</sup>, J.C. Eckardt <sup>a</sup>

<sup>a</sup> Centro Atómico Bariloche and Instituto Balseiro, Comisión Nacional de Energía Atómica, 8400 San Carlos de Bariloche, Argentina

<sup>b</sup> Instituto de Física da Universidade Federal do Rio Grande do Sul, Avenida Bento Gonçalves 9500, C.P. 15051, CEP 91501-970 Porto Alegre, Brazil

<sup>c</sup> Instituto de Física, Universidade de São Paulo, C.P. 66318, 05315-970 São Paulo, Brazil

### ARTICLE INFO

#### Article history:

Received 7 May 2012

Received in revised form 13 June 2012

Available online 23 June 2012

#### Keywords:

Stopping power

Helium energy loss

Aluminum oxide

### ABSTRACT

In the present work, we report experimental results of He stopping power into  $\text{Al}_2\text{O}_3$  films by using both transmission and Rutherford backscattering techniques. We have performed measurements along a wide energy range, from 60 to 3000 keV, covering the maximum stopping range. The results of this work are compared with previously published data, showing a good agreement for the high-energy range, but evidencing discrepancies in the low-energy region. The existing theories follow the same tendency: good theoretical-experimental agreement for higher energies, but they failed to reproduce previous and present results in the low energy regime. On the other hand it is interesting to note that the semi-empirical SRIM code reproduces quite well the present data.

© 2012 Elsevier B.V. All rights reserved.

## 1. Introduction

Alumina is an important material broadly used in mechanical, optical, optoelectronics or microelectronic applications due to its excellent chemical resistance, good mechanical strength, high hardness, transparency, high abrasion and corrosion resistance. All these remarkable properties make  $\text{Al}_2\text{O}_3$  a typical choice as a matrix/substrate for optical waveguide amplifiers in integrated systems [1], solid-state lasers or thin-film devices [2,3]. Also, the electronic properties of  $\text{Al}_2\text{O}_3$  films allow their use as gate dielectric for field-effect transistors [4]; whereas the capability to insert nanocomposites in alumina matrices suggests potential applications in nanoscale memory devices.

On the other hand, the study of the energy deposition of energetic ions in matter is a problem of interest for basic and applied research in many areas, such as ion implantation, ion beam analysis and modification of materials, radiation damage, radiation therapy or space research [5–8]. Therefore due to the importance of alumina films, it is desirable to know accurately their stopping power in a wide range of ion energies.

The stopping power of He in  $\text{Al}_2\text{O}_3$  was first studied in the seventies by L'Hoir et al. [9] and Thomas [10]. More results were reported by other authors, using the transmission technique [11,12]. Two theoretical works were also published, where the stopping power of some light ions and in particular He in alumina were investigated. This was done in order to study departures from the Bragg's rule [13,14]. Finally, in the last decade, two works were

published in which, by using the Bayesian approach, new stopping power values in alumina were reported [15,16].

Despite this large amount of data, there is still some dispersion among the different experimental results, mainly in the low-energy regime. Moreover, the two different theoretical approaches [13,14] were not able to reproduce the low-energy range data. In addition the semi-empirical predictions of the SRIM algorithm [17] do not fully reproduce the previously published data.

Based on the above-mentioned features, we have undertaken the present experimental work in order to revise the He in  $\text{Al}_2\text{O}_3$  stopping data. With this purpose we have measured the stopping in a wide energy range interval, from 60 up to 3000 keV. These measurements were done using two techniques: the Rutherford backscattering (RBS) for the higher energies (above 170 keV) and the transmission technique for the lower ones. The results are compared with the previously published data, as well as, with the theoretical predictions and the SRIM 2010 semi-empirical calculations [17].

## 2. Experimental method

In order to determine the stopping power of He in  $\text{Al}_2\text{O}_3$ , we have used two experimental techniques: the RBS for the higher projectile energies and the foil transmission for the lower ones. The consistency of both techniques was checked in a common energy range interval from 170 to 200 keV.

For the RBS experiments, the  $\text{Al}_2\text{O}_3$  films were prepared by radio frequency magnetron sputtering using a commercial target and  $\text{O}_2/\text{Ar}$  mixture as a sputtering gas. The sample has a nominal purity of 99.99%. Films of thicknesses of 43, 72 and 117 nm were deposited

\* Corresponding author. Tel.: +55 51 33086551; fax: +55 51 33087286.

E-mail address: [behar@if.ufrgs.br](mailto:behar@if.ufrgs.br) (M. Behar).

on a gold film that was previously evaporated on a silicon substrate. This is due to the fact that the Si signal of the substrate overlaps with the  $\text{Al}_2\text{O}_3$  one. Therefore, with the present substrate/films structure (Si/Au/ $\text{Al}_2\text{O}_3$ ), we used the high-energy edge of the Au signal, which corresponds to projectiles backscattered in the outermost layer of Au. Those projectiles, in addition to the elastic energy loss in the backscattering event, also lose energy in the inward and outward paths of the  $\text{Al}_2\text{O}_3$  film. The ion energy reduction  $\Delta E$  in the alumina film can be determined by performing a comparison with the energy of ions backscattered at the Au surface, as shown in Fig. 1. The thicknesses of the  $\text{Al}_2\text{O}_3$  films were determined by using a 3 MeV He and a 1 MeV proton beams. For those energies, the stopping of He and proton in  $\text{Al}_2\text{O}_3$  are already known and well reproduced by SRIM [17]. By using the corresponding SRIM stopping powers, we have found thickness discrepancies less than 3%.

The RBS technique was used in the 170–3000 keV energy range. The total energy resolution of the system was 12 keV (FWHM) and the ion beam was provided by the 500 kV ion implanter and the 3 MV Tandetron accelerator of the Instituto de Física da Universidade Federal do Rio Grande do Sul (IF-UFRGS).

The samples were mounted on a four-axis goniometer and the detector was fixed at  $120^\circ$  with respect to the incident ion beam. For each incident energy, four backscattering spectra were recorded at the angles of incidence  $\theta_1 = 0^\circ, 20^\circ, 40^\circ$  and  $60^\circ$  with respect to the beam direction. The choice of the films was done taking into account the beam energy. In some cases, for a given energy, two different films were used and the obtained results were consistent.

For each studied beam energy and geometry, the corresponding  $\Delta E$  value was determined. Taking into account the target thickness  $t$ , we have obtained, for each beam energy, four equations in the form:

$$\frac{\Delta E}{t} = \frac{K}{\cos \theta_1} \frac{dE}{dx} \Big|_{E_{\text{in}}} + \frac{1}{\cos \theta_2} \frac{dE}{dx} \Big|_{E_{\text{out}}} \quad (1)$$

where  $K$  is the kinematic factor,  $\theta_1$  is the angle between the incident beam and the target's normal, and  $\theta_2$  is the angle between the target's normal and the detector direction [18]. The energies  $E_{\text{in}}$  and  $E_{\text{out}}$  were obtained using the energy-loss ratio method [8] in the mean-energy approximation. The obtained system of equations

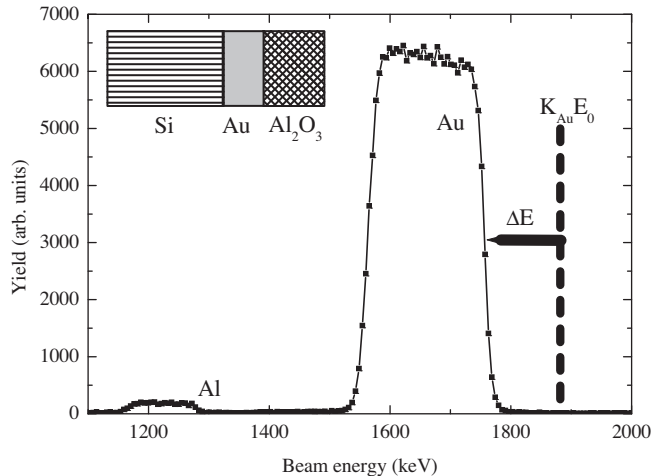


**Fig. 1.** Rutherford backscattering spectrum taken with a He ion beam at 2 MeV. The angle of the incident ion beam direction with the sample normal is  $40^\circ$ , and the angle with the detector is  $120^\circ$ . The surface Al and the Au layer signals are depicted. The high-energy edge of the Au peak is displaced toward lower energies with respect to a backscattering event occurring at an Au surface due to the energy loss in the 117 nm  $\text{Al}_2\text{O}_3$  film.

for  $dE/dx|_{E_{\text{in}}}$  and  $dE/dx|_{E_{\text{out}}}$  can be solved by a graphical or an analytical method. Further details of this procedure are given in Ref. [18]. Proceeding in this way we have obtained the He stopping power for all the studied energy range for backscattering measurements (170–3000 keV). The breakdown of the single scattering model to a plural scattering regimen should not change significantly the energy transfer  $\Delta E$  measurements since the projectile entrance and exit angles were kept below  $60^\circ$  [19].

It should be mentioned that the main source of errors in the RBS reported values of the stopping power relies on the target thickness determination. The graphical solution of Eq. (1) for the four geometries used in the RBS experiments added just a small uncertainty, about 2% for higher energy values. Then, the total uncertainty in the stopping cross section determination is at most about 4% in the high energy range. For further experimental details, we refer to Ref. [20].

The energy loss determinations with energies between 60 and 200 keV were done at the Atomic Collision Laboratory of the Centro Atómico Bariloche (CAB), employing the transmission method using a thin self-supporting foil. The self-supported foils were made by electron-gun evaporation under clean vacuum conditions on a very smooth plastic substrate, which was subsequently dissolved. In order to avoid systematic uncertainties, we have used the obtained low energy RBS data to renormalize the transmission energy-loss data for energies near 200 keV. The mean foil thickness of the  $\text{Al}_2\text{O}_3$  targets was 33 nm.

The ion beams were generated by an electrostatic accelerator with an rf ion source followed by focusing and mass selection stages. The  $\text{Al}_2\text{O}_3$  foils were mounted on a movable holder to allow energy measurements of the direct beam, and the beam transmitted through the target. The energy analysis was performed by an electrostatic analyser with 0.3% FWHM resolution positioned in the forward beam direction. The charging up from the targets by the projectiles was avoided by a low energy electron shower.

### 3. Results

The complete set of results measured at CAB and IF-UFRGS is shown in Fig. 2. Some representative previously published results [9–12,15] are shown in the same figure. In addition we also display the stopping power predictions of He in  $\text{Al}_2\text{O}_3$  from the semi-empirical SRIM 2010 code.

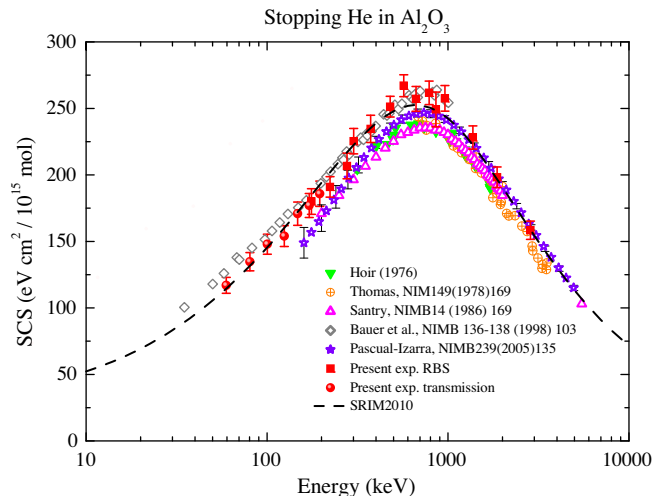


**Fig. 2.** Present and previously published stopping power data. In addition, the prediction of the SRIM 2010 code is also shown.

At variance with some previously published results, in the present work we have mostly used the RBS technique to determine the experimental stopping values. This was done in a wide energy range, from 170 to 3 MeV going through the maximum of the curve. The use of the foil transmission technique for energies below 200 keV allows us to explore an energy region that is not so suitable for the RBS technique.

An observation of Fig. 2 allows us to compare the present and previously published results. For energies higher than 1.5 MeV all the reported results agree with the present one. However, near the maximum stopping power and for lower energies, the present values show a tendency to be higher than those published by L'Hoir et al. [9], Thomas [10], Santry and Werner [11] and Pascual-Izarra et al. [15]. For lower energies the discrepancies became larger and completely out of the experimental uncertainties. On the other hand our results are in good agreement with those reported by Bauer et al. [12] for almost all the energy range (35–1000 keV) covered by the authors.

From a theoretical point of view, there are two published reports. In the first one by Peñalba et al. [13], it was used a dielectric function to estimate the target valence electron contribution to the stopping power, together with a formalism that takes into account charge state effects. In addition for lower energies, they have introduced an electron gas model with an effective number of electrons and a nonlinear description within the density-functional theory. The same happens with a theoretical work by Heredia-Avalos et al. [14]. The evaluation was also done in the framework of the dielectric formalism. The target properties were described by means of a combination of Mermin-type of energy loss functions that characterize the response of valence-band electrons, together with generalized oscillator strengths to take into account the ionization of inner-shell electrons. Both theories reproduce well the high-energy experimental values but does not reproduce well the low-energy ones. For energies lower than 200 keV, both models underestimate the experimental results showed in Ref. [12] and the present ones. Finally it should be stated that the energy dependence of the present results are well reproduced by the semi-empirical SRIM 2010 code calculations – see Fig. 2. The agreement is good through all the energy range covered by the present work.

#### 4. Summary

In the past, the He stopping power in  $\text{Al}_2\text{O}_3$  was experimentally studied by several authors. However, the present work is the first one that covers a so wide energy range that goes from 60 up to 3000 keV. To this end we have combined two techniques: the transmission for the lower energy (60–200 keV) range and the RBS from 170 up to 3000 keV. Comparison with previously published data [9–11,15,16] indicates good agreement at higher energies, not so good around the maximum of the stopping power and rather poor for lower energies. On the other hand a general good agreement was observed with the results of Bauer et al. [12], however it should be stated that they have performed their

measurements in smaller energy range (from 35 up to 1000 keV). Concerning the two theoretical works published up to the present, they reproduce quite well the high-energy region of the experimental results but fail in their predictions for the lower stopping power energies.

Finally we should emphasize – as shown in Fig. 2 – that an agreement on the energy loss behavior was obtained between our results and the predictions of the semi-empirical SRIM 2010 code. However we expect that in the future a first principles theory would be able to reproduce both: the low energy range results as well as the high energy ones.

#### Acknowledgments

This work has been financially supported by the Brazilian Conselho Nacional de Desenvolvimento Científico e Tecnológico (CNPq), and the ANPCYT of Argentina (Project PICT 903/07). E.D.C. acknowledges support from the Consejo Nacional de Investigaciones Científicas y Técnicas (CONICET), Argentina.

#### References

- [1] M.J. de Castro, A. Suárez-García, R. Serna, C.N. Afonso, J.G. López, *Opt. Mater.* 29 (2007) 539.
- [2] B. Handke, J.B. Simonsen, M. Bech, Z. Li, P.J. Miller, *Surf. Sci.* 600 (2006) 5123.
- [3] T. Murakami, J.H. Ouyang, S. Sasaki, K. Umeda, Y. Yoneyama, High-temperature tribological properties of spark-plasma-sintered  $\text{Al}_2\text{O}_3$  composites containing barite-type structure sulfates, *Tribol. Int.* 40 (2007) 246.
- [4] K. Vanbesien, P. De Visschere, P.F. Smet, D. Poelman, *Thin Solid Films* 514 (2006) 323.
- [5] Y. Li, S. Zhang, Y. Liu, T.P. Chen, T. Sritharan, C. Xu, J. Nanosci. Nanotechnol. 9 (2009) 1–5.
- [6] H. Bernas (Ed.), *Materials Science with Ion Beams*, Topics in Applied Physics, vol. 116, Springer, Heidelberg, 2009.
- [7] G. García Gómez-Tejedor, M.C. Fuss (Eds.), *Radiation Damage in Biomolecular Systems* in the series *Biological and Medical Physics, Biomedical Engineering*, Springer, Heidelberg, 2012.
- [8] D.C. Turner, N.F. Mangelson, L.B. Rees, *Nucl. Instr. Meth. B* 103 (1995) 28; J.E. Turner, *Atoms, Radiation and Radiation Protection*, Wiley-VCH, Weinheim, 2007.
- [9] A. L'Hoir, C. Cohen, G. Amsel, *Ion Beam Surface Layer Analysis*, Plenum Press, New York, 1975, p. 965.
- [10] J.P. Thomas, M. Fallavier, *Nucl. Instr. Meth. B* 149 (1978) 169.
- [11] C. Santry, R.D. Werner, *Nucl. Instr. Meth. B* 14 (1986) 169. and references therein.
- [12] P. Bauer, R. Golser, D. Semrad, P. Meier-Komor, F. Aumayr, A. Arnau, *Nucl. Instr. Meth. B* 136–138 (1998) 103. and references therein.
- [13] M. Peñalba, J.I. Juaristi, E. Zarate, A. Arnau, P. Bauer, *Phys. Rev. A* 64 (2001) 012902.
- [14] Santiago Heredia-Avalos, Rafael García-Molina, Jose M. Fernandez-Varea, Isabel Abril, *Phys. Rev. A* 72 (2005) 053902.
- [15] C. Pascual-Izarra, M. Bianconi, N.P. Barradas, A. Climent-Font, G. García, J. Gonzalo, C.N. Afonso, *Nucl. Instr. Meth. B* 219–220 (2004) 268.
- [16] C. Pascual-Izarra, N.P. Barradas, G. García, A. Climent-Font, *Nucl. Instr. Meth. B* 23 (9) (2005) 135.
- [17] J.F. Ziegler, J.P. Biersack, SRIM 2010. The Stopping and Range of Ions in the Matter, version 2010, code available from <<http://www.srim.org>>.
- [18] W.K. Chu, J.W. Mayer, M.A. Nicolet, *Backscattering Spectrometry*, Academic, New York, 1978.
- [19] W. Eckstein, M. Mayer, *Nucl. Instr. Meth. B* 15 (3) (1999) 337.
- [20] E.D. Cantero, R.C. Fadanelli, C.C. Montanari, M. Behar, J.C. Eckardt, G.H. Lantschner, *Phys. Rev. A* 79 (2009) 042904.